RSC Advances

PAPER

View Article Online
View Journal | View Issue

Cite this: *RSC Adv.*, 2022, **12**, 36028

The influence of $(H_2O)_{1-2}$ in the HOBr + HO_2 gas-phase reaction†

Yunju Zhang, *[ab] Yongguo Liu,[b] Meilian Zhao,[c] Yuxi Sun[a] and Shuxin Liu*[a]

Received 3rd October 2022
Accepted 1st November 2022

DOI: 10.1039/d2ra06204f

rsc.li/rsc-advances

The HOBr + HO_2 reaction in the absence of water has three different channels for the abstraction of H to generate the corresponding products. The dominant channel is the generation of BrO + H_2O_2. The introduction of water molecules influences this dominant reaction *via* the way the reactants interact with the water molecules. The addition of water molecules decreases the energy barrier and increases the rate coefficient of the reaction. Interestingly, water works as a catalyst and we obtain BrO + H_2O_2, like in the reaction without water, or the water works as a reactant and we obtain products other than BrO + H_2O_2. The rate coefficients of the HOBr + HO_2 reaction in the presence of water are calculated to be faster than the reaction in the absence of water. However, other pathways in the presence of water are slower than the reaction in the absence of water. The water-assisted effective rate coefficients for the HOBr + HO_2 reaction are also larger than those for the reaction in the absence of water. The influence of a water dimer is not as important when compared with one water molecule. In summary, a single water molecule has a positive catalytic influence in enhancing the HOBr + HO_2 reaction.

1. Introduction

Ozone is an important component gas in the Earth's atmosphere which is mainly distributed in the stratosphere and troposphere. The hole in the ozone layer is the area where the ozone concentration in the stratosphere decreases greatly. Now, more and more people have realized that the ozone loss caused by halogen catalysis plays a significant role in the stratosphere and troposphere. However, there is no quantitative model to simulate the ozone budget in these regions,[1,2] and it is evident that this deficiency is mainly due to our comprehension of atmospheric halogen chemistry.[3] Obviously, halogens can participate in many catalytic cycles of gas-phase ozone destruction. Such cycles involve the generation and photolysis of hypohalic acid (HOX):[4]

$$XO + HO_2 \rightarrow HOX + O_2 \ (X = Cl, Br)$$

$$HOX + h\nu \rightarrow OH + X$$

$$OH + O_3 \rightarrow HO_2 + O_2$$

$$X + O_3 \rightarrow XO + O_2$$

$$\text{Net: } 2O_3 \rightarrow 3O_2$$

This cycle combines rare hydrogen (HO_x) chemistry with halogen chemistry in the atmosphere, which is particularly significant for levels of chlorine in the lower stratosphere and bromine in the troposphere.[5] Due to the disadvantageous effect of HOX on stratospheric ozone, HOX makes a significant impact on atmospheric chemistry. HOBr is considered to be a provisional reservoir of BrO_x substances in the stratosphere. Moreover, as a significant source of atmospheric bromine, the reaction of HOBr with HO, NO, and HO_2 has a significant impact on atmospheric chemistry.[6–8] HO_2 also plays an important role in the atmospheric oxidation of the volatile organic compounds (VOCs),[9,10] particularly as the ratio of HO_2 to OH radicals is high. In addition, the generation of many secondary pollutants such as ozone, oxygenated organic compounds, peroxyacetyl nitrates and secondary organic aerosols is closely related to the presence of HO_2 in the atmosphere.[11,12] Consequently, the reaction between HO_2 and HOBr has a significant impact on the process of atmospheric change and climate change.

In 2012, Dixon-Lewis *et al.*[13] investigated the HO_2 + HOBr → H_2O_2 + BrO reaction, and observed a rate coefficient of this channel to be $k = 1.03T^{3.55}\exp(-6590/T)$ cm^3 mol^{-1} s^{-1}. So far, there have not been any other experimental and theoretical investigations on the HO_2 + HOBr reaction. However, these previous investigations did not consider the effect of water

[a]*Key Laboratory of Photoinduced Functional Materials, Mianyang Normal University, Mianyang 621000, PR China. E-mail: zhangyj010@nenu.edu.cn; 394199822@qq.com; Fax: +86 816 2200819; Tel: +86 816 2200064*

[b]*Beijing Key Laboratory of Flavor Chemistry, Beijing Technology and Business University (BTBU), Beijing 100048, PR China*

[c]*College of Medical Technology, Chengdu University of Traditional Chinese Medicine, Liutai Avenue, Wenjiang District, Chengdu, PR China*

† Electronic supplementary information (ESI) available. See DOI: https://doi.org/10.1039/d2ra06204f

vapor on the reaction of HO_2 + HOBr. Numerous investigations have found that water vapors can combine with HO, O_3, HO_2, BrO and HNO_3 in the atmosphere[14–19] to generate $O_3\cdots H_2O$, $HO\cdots H_2O$, $ClO\cdots H_2O$ $HO_2\cdots H_2O$ and $HNO_3\cdots H_2O$ complexes which possess a cyclic structure and are extraordinarily stable. At the same time, the participation of water in reactions could improve the stability of intermediates and decrease the energy barrier of transition states required to catalyze the reactions.[20–25] In the atmosphere, over 30% of HO_2 radicals could combine with water.[17] These circumstances aroused our attention for the simulation of the ternary system $H_2O\cdots HO_2\cdots$HOBr, in which a water molecule serves as a catalyst.

In the present work, we analyzed the influence of a single molecule of water on the reaction of HO_2 + HOBr *via* the investigation of the reaction mechanism and rate coefficient for the reaction in the absence and presence of water. The results gained are helpful to comprehend the influence of water on atmospheric reactions.

2. Computational methods

The B3LYP[26,27] method and 6-311++G(d,p) basis set were used to obtain the geometric parameters of all the stationary points. Harmonic vibrational frequency calculations were performed at the same level of theory in order to determine the nature of the various stationary points, as well as the zero-point-energy (ZPE) corrections. The transition states were verified by intrinsic reaction coordinate (IRC) calculations to connect the designated reactants and products.[28,29] Based on the optimized geometries at the B3LYP/6-311++G(d,p) level of theory, a CCSD(T)[30]//cc-pVTZ method was employed to obtain accurate single point energies. All calculations were carried out using the GAUSSIAN 09 program package.[31] The rate coefficients of the BrO + HO_2 reaction were employed by the KisThelP program,[32] which is based on the Transition State Theory (TST) with Wigner tunneling correction. The detailed process of calculating the rate coefficient, according to a study by Shiroudi,[33] is in the ESI.†

3. Results and discussion

3.1 The mechanism of the reaction of HOBr with HO_2 in the absence of water

The potential energy surface (PES) obtained at the CCSD(T)/cc-pVTZ//B3LYP/6-311++G(d,p) level of theory for the HOBr + HO_2 reaction in the absence of a water molecule involves three different channels (channel 1, channel 2 and channel 3), which are presented in Fig. 1. The channel that generates H_2O_2 and

Table 1 The relative energies including electronic energies ($\Delta E_{298\ K}$), enthalpies $\Delta H_{298\ K}$, and Gibbs free energies $\Delta G_{298\ K}$ for the HOBr + HO_2 reaction in the absence of water, units: kcal mol^{-1}

System	$\Delta E_{298\ K}$	$\Delta H_{298\ K}$	$\Delta G_{298\ K}$
HOBr + HO_2	0.00	0.00	0.00
COMR1	−4.07	0.81	3.09
TS1	19.88	23.96	29.22
TS2	29.43	33.85	38.03
TS3	44.24	48.28	54.30
TS4	34.73	38.70	44.94
COMP1	7.85	12.71	15.18
BrO + H_2O_2	11.74	11.65	12.41
Br + O_2 + H_2O	3.30	9.23	−1.10
OBrO + H_2O	−2.96	2.14	−1.93

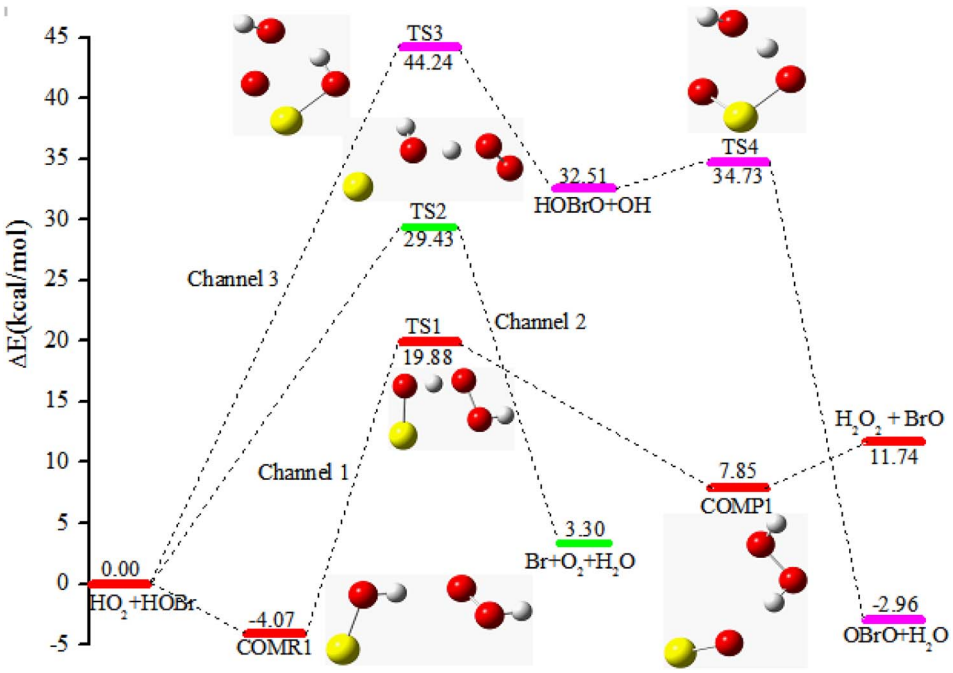

Fig. 1 The PES of the HOBr + HO_2 reaction in the absence of water at the CCSD(T)/cc-pVTZ//B3LYP/6-311++G(d,p) level of theory (energies in kcal mol^{-1}).

BrO starts from a pre-reactive complex (COMR1), which is stabilized through a hydrogen bond (1.942 Å). The energy of COMR1 is −4.07 kcal mol^{-1} (see Table 1) and it can pass through TS1 to generate a post-reactive complex (COMP1) and then dissociate to H_2O_2 and BrO surmounting a barrier of 23.95 kcal mol^{-1}. The geometry of the transition state (TS1) for the HO_2 + HOBr → H_2O_2 + BrO reaction was studied at the B3LYP/6-311+G(d,p) level of theory by Dixon-Lewis *et al.*[13] The dihedral angles and frequencies are very consistent with our calculations. The dihedral angles HOOH, OOHO and OHOBr are 126.8°, 84.5° and 79.4°, which are agreement with our calculated results of 126.7°, 84.5° and 79.2°, respectively. The frequencies are 1194*i*, 72, 81, 283, 332, 515, 674, 997, 1120, 1338, 1553, 3595 cm^{-1}, which are in agreement with our calculated results of 1232*i*, 73, 83, 292, 341, 533, 697, 1031, 1157, 1383, 1604, 3717 cm^{-1}. Channel 2 involves the O atom in HOBr extracting the H atom in HO_2 whilst breaking the O–Br bond to generate Br + O_2 + H_2O *via* TS2. The barrier of HOBr + HO_2 → TS2 → Br + O_2 + H_2O is 29.43 kcal mol^{-1}, which is higher than that of channel 1 by 5.48 kcal mol^{-1}. In addition, the terminal O atom of HO_2 can interact with the Br atom of HOBr resulting in HOBrO + OH *via* TS3 and overcoming a rather high barrier of 44.24 kcal mol^{-1}. Subsequently, the OH radical can further extract an H atom from HOBrO to form OBrO + H_2O *via* TS4 with

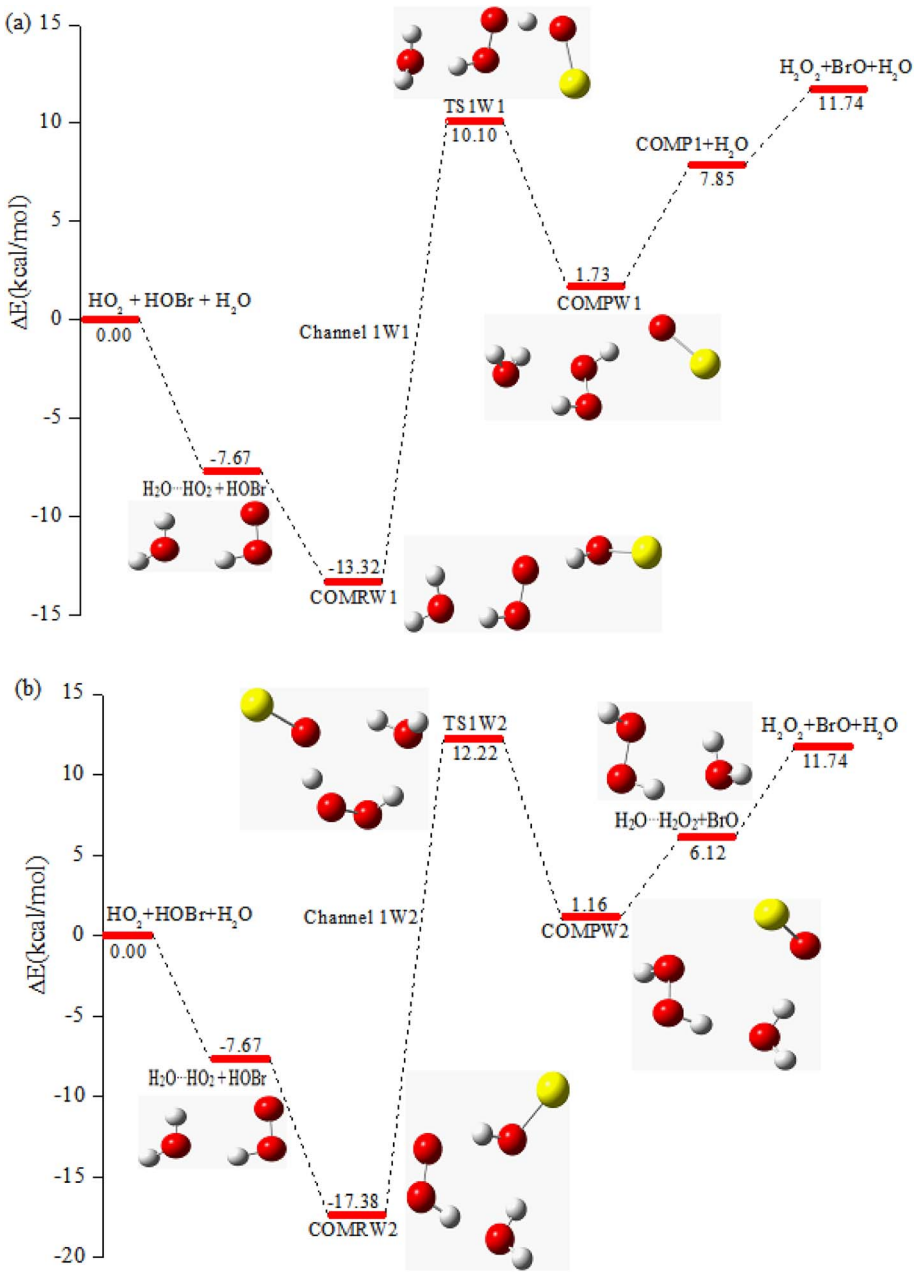

Fig. 2 The PESs of the HOBr + HO_2 reaction in the presence of water *via* the $H_2O\cdots HO_2$ + HOBr channel at the CCSD(T)/cc-pVTZ//B3LYP/6-311++G(d.p) level of theory (energies in kcal mol^{-1}), (a) $H_2O\cdots HO_2$ + HOBr→COMRW1→products, (b) $H_2O\cdots HO_2$ + HOBr→COMRW2→products.

a barrier of 2.22 kcal mol^{-1}. Although channel 3 is exothermic by 2.96 kcal mol^{-1}, this channel cannot take place quickly owing to the high barrier of the HOBr + HO_2 → TS3 → OBrO + H_2O reaction. Thus, the three channels for abstraction are not important for the HOBr + HO_2 reaction in the absence of a water molecule due to their high barrier heights and unstable products.

3.2 The mechanism of the reaction of HOBr with HO_2 in the presence of one water molecule

To study the influence of one water molecule on the abstraction of H in the HOBr + HO_2 reaction in the atmosphere, different channels have been investigated. The participation of one water molecule complicates the abstraction channels of the HOBr + HO_2 reaction. Since it is impossible for the collision of three isolated molecules (including HOBr, HO_2 and H_2O) to occur simultaneously, they will firstly generate a two-body complex, and then generate a three-body complex by the collision between the third species and the two-body complex. When one water molecule participates, it can interact with HOBr and HO_2 through hydrogen bonds to generate the corresponding three dimer complexes, namely, $H_2O\cdots HO_2$, $H_2O\cdots$HOBr and HOBr$\cdots H_2O$. The energies of these three dimer complexes are −7.67, −6.13 and −3.08 kcal mol^{-1}, respectively. These dimer complexes can further react with the third species to generate the corresponding three-body complexes (COMRW1, COMRW2, COMRW3, COMRW4 and COMRW5). Hence, when a water molecule is added into the channel for the generation of BrO + H_2O_2 from the reaction of HOBr + HO_2, the PESs seem to be more complex resulting in five different bimolecular reactions channels (marked as channel 1W1, channel 1W2, channel 1W3A, channel 1W3B, channel 1W4 and channel 1W5). Therefore, to investigate the influence of a water molecule on the title reaction under atmospheric conditions, five water auxiliary channels were studied.

3.2.1 The channel for the $H_2O\cdots HO_2$ + HOBr reaction. As shown in Fig. 2a and b, the $H_2O\cdots HO_2$ + HOBr reaction starts with the generation of pre-reactive complexes COMRW1 and COMRW2 where the binding energies with respect to the separate reactants are −13.32 and −17.38 kcal mol^{-1}, respectively. Starting from COMRW1, the reaction takes place through TS1W1 to generate the post-reactive complex COMPW1 (1.73 kcal mol^{-1}) which then decomposes to COMP1 + H_2O. The barrier of COMRW1 → TS1W1 → COMPW1 is 23.42 kcal mol^{-1}. Complex COMRW1 is more stable than COMR1 by 9.25 kcal mol^{-1}. During the process in channel 1W1, the water just serves as a solvent and does not enter into the reaction. As listed in Table 2, compared with the reaction in the absence of a water molecule, the barrier is decreased by 0.53 kcal mol^{-1}, which shows that the water molecule in channel 1W1 has a small positive influence on the HO_2 + HOBr reaction. In addition, starting from complex COMRW2, the reaction (channel 1W2) occurs *via* TS1W2 to generate the post-reactive complex COMPW2 which decomposes to $H_2O\cdots H_2O_2$ + BrO. The energies of COMRW2 and COMPW2 are 4.06 and 0.57 kcal mol^{-1} lower than those of COMRW1 and COMPW1, respectively. The role of water in this reaction is also to act as a solvent. The barrier of COMRW2 → TS1W2 → COMPW2 is 29.60 kcal mol^{-1}, which is 6.18 and 5.65 kcal mol^{-1} higher than those of channel 1W1 and the reaction in the absence of water, respectively. Therefore, the presence of water in pathway 1W2 does not accelerate the HOBr + HO_2 reaction.

Table 2 The relative energies including electronic energies ($\Delta E_{298\ K}$), enthalpies $\Delta H_{298\ K}$, and Gibbs free energies $\Delta G_{298\ K}$ for the reactions stemming from $H_2O\cdots HO_2$ + HOBr, $H_2O\cdots$HOBr + HO_2 and HOBr$\cdots$ H_2O + HO_2, units: kcal mol^{-1}

System	$\Delta E_{298\ K}$	$\Delta H_{298\ K}$	$\Delta G_{298\ K}$
HOBr + HO_2 + H_2O	0.00	0.00	0.00
$H_2O\cdots HO_2$ + HOBr	−7.67	−3.47	−0.50
$H_2O\cdots$HOBr + HO_2	−6.13	−6.42	0.47
HOBr$\cdots H_2O$ + HO_2	−3.08	−3.11	4.11
$H_2O\cdots H_2O_2$ + BrO	6.12	5.48	14.21
$H_2O\cdots$BrO + H_2O_2	9.16	8.97	15.08
BrO$\cdots H_2O$ + H_2O_2	7.81	7.36	15.63
COMRW1	−13.32	−8.82	1.10
TS1W1	10.10	13.94	26.46
COMPW1	1.73	6.02	17.46
COMRW2	−17.38	−13.78	0.14
TS1W2	12.22	15.83	29.89
COMPW2	1.16	5.58	16.66
COMRW3	−10.01	−5.43	3.77
TS1W3A	24.46	27.43	43.07
TS1W3B	28.02	31.11	46.17
COMPW3	1.14	5.54	16.84
COMRW4	−17.46	−13.89	0.16
TS1W4	−5.47	−3.11	13.90
COMRW5	−6.58	−1.58	7.63
TS1W5	13.44	17.66	30.05
COMPW5	3.28	7.84	18.23
BrO + H_2O_2 + H_2O	11.74	11.65	12.41

3.2.2 The channel for the $H_2O\cdots$ HOBr + HO_2 reaction. Fig. 3(a) and (b) present the PESs for the reaction of $H_2O\cdots$HOBr + HO_2. Compared with the direct hydrogen transfer extraction mechanism (channel 1W1 and channel 1W2), channel 1W3A and channel 1W3B refer to a synchronous doublet proton transfer mechanism where the water molecule enters into the reaction in both channels. The reactions in channel 1W3A and channel 1W3B start from complex COMRW3 with a binding energy of −10.01 kcal mol^{-1}, when compared with the individual molecules. COMRW3 is stabilized through two hydrogen bonds (1.962 and 1.773 Å). After the generation of COMRW3, the reaction proceeds *via* TS1W3A or TS1W3B to generate post-reactive complex COMPW3 and decompose to $H_2O\cdots$BrO + H_2O_2, which is 11.15 kcal mol^{-1} higher than COMRW3. The water in TS1W3A and TS1W3B serves as a bridge for hydrogen transfer. The barriers of COMRW3 → TS1W3A → COMPW3 and COMRW3 → TS1W3B → COMPW3 are 34.47 and 38.03 kcal mol^{-1}, respectively, which are 10.52 and 14.08 kcal mol^{-1} higher than that of the channel absent of a water molecule, respectively. These results show that the water molecule serves as an inhibitor that increases the energy barrier. Hence, channel 1W3A and channel 1W3B would be unlikely to take place in a real atmosphere.

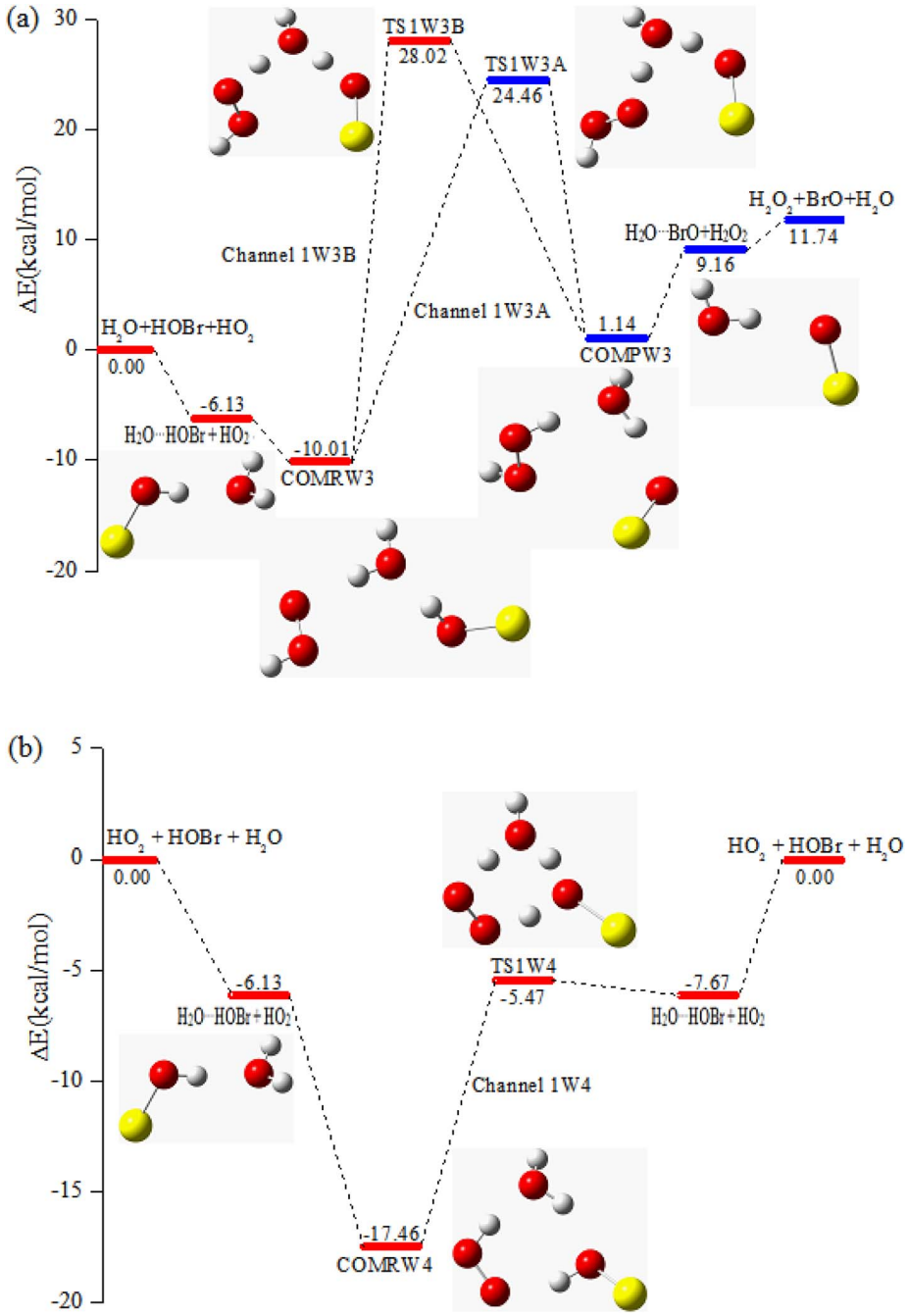

Fig. 3 The PESs of the HOBr + HO_2 reaction in the presence of water *via* the $H_2O\cdots HOBr + HO_2$ channel at the CCSD(T)/cc-pVTZ//B3LYP/6-311++G(d.p) level of theory (energies in kcal mol^{-1}), (a) $H_2O\cdots HOBr + HO_2 \rightarrow$ COMRW3 $\rightarrow$ products, (b) $H_2O\cdots HOBr + HO_2 \rightarrow$ COMRW4 $\rightarrow$ products.

Another fascinating discovery of this work is the finding of a synchronous triplet-proton transfer mechanism. Water is also involved in channel 1W4, which starts from one pre-reactive complex COMRW4 with three hydrogen bonds (1.846, 1.831 and 1.655 Å). The stabilization energy of COMRW4 is −17.46 kcal mol^{-1}, which is lower than COMR1 by 13.39 kcal mol^{-1}. Subsequently, COMRW4 can proceed through a seven-membered-ring (O–H–O–O–H–O–H) transition state TS1W4 to generate the products $H_2O\cdots HO_2$ and HOBr. TS1W4 is a three hydrogen-atom transfer mechanism where the water molecule serves as a bridge. The barrier of the COMRW4 → TS1W4 → $H_2O\cdots HO_2$ + HOBr process is 11.99 kcal mol^{-1}, which is 11.96 kcal mol^{-1} lower than the reaction in the absence of water, demonstrating that channel 1W4 may be of significance for the HO_2 + HOBr + H_2O reaction by increasing the stability of the complex and reducing the barrier height.

3.2.3 The channel for the HOBr$\cdots H_2O$ + HO_2 reaction. The products of the $HOBr\cdots H_2O$ + HO_2 reaction could be obtained

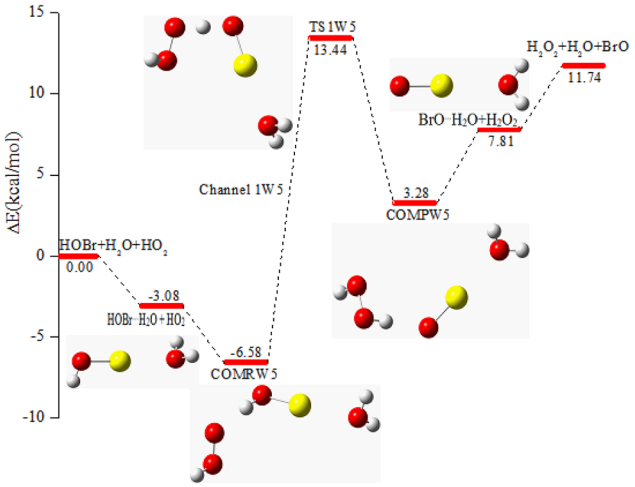

Fig. 4 The PES of the HOBr + HO_2 reaction in the presence of water *via* the HOBr···H_2O + HO_2 channel at the CCSD(T)/cc-pVTZ//B3LYP/6-311++G(d.p) level of theory (energies in kcal mol^{-1}).

through channel 1W5 (see Fig. 4). The first step of channel 1W5 is the generation of a pre-reactive complex COMRW5. COMRW5 involves a hydrogen bond and halogen bond, with a binding energy of −6.58 kcal mol^{-1}. Subsequently, the reaction proceeds through TS1W5 to generate COMPW5 and then decompose to BrO···H_2O + H_2O_2. The energy of COMPW5 is higher than the reactants by 3.28 kcal mol^{-1}, which is 9.86 kcal mol^{-1} higher than COMRW5. The barrier of COMRW5 → TS1W5 → COMPW5 is 20.02 kcal mol^{-1}, which is 3.93 kcal mol^{-1} lower than that of the channel absent of water. This suggests that channel 1W5 might occur more easily than channel 1. Finally, BrO, H_2O_2 and H_2O were released to the gas phase.

3.3 The mechanism in the presence of a water dimer

As shown in Fig. 5, when a water dimer is present in the entrance channel, one cyclic three-body complex $2H_2O$···HO_2 is formed. Subsequently, *via* the interaction of $2H_2O$···HO_2 with HOBr, two pre-reaction complexes COMRWW1 and COMRWW2 are generated with binding energies of −7.13 and −10.23 kcal mol^{-1}, respectively. Starting from COMRWW1, the reaction generates the corresponding product complex COMPWW1 through transition state TS1WW1 before releasing the products H_2O_2 and BrO (channel 1WW1). In channel 1WW2, the reactants move from COMRWW2 through transition state TS1WW2 to generate $2H_2O$···HO_2 + HOBr which then decomposes to the final products. channel 1WW3 also starts from COMRWW2 and can also directly generate the final products H_2O_2 and BrO through transition state TS1WW3. The energies of TS1WW1, TS1WW2 and TS1WW3 are 17.87, 5.29 and 34.14 kcal mol^{-1} higher than the $2H_2O$···HO_2 + HOBr reactants, which is similar to channel 1W1 and channel 1W3B (17.77 and 34.15 kcal mol^{-1}). However, TS1WW2 is 5.29 kcal mol^{-1} higher in energy relative to the $2H_2O$···HO_2 + HOBr reactants, which is higher than that of channel 1W4 (−0.66 kcal mol^{-1}). In addition, the configurations of the core complexes in COMRWW1 and TS1WW2 are similar to those in COMRW4 and TS1W4. The barrier height of channel 1WW2 is 13.87 kcal mol^{-1} with respect to the COMRWW2, which is 11.99 kcal mol^{-1} higher than the energy barrier of COMRW4 → TS1W4 → H_2O···HO_2 + HOBr. Thus, the effect of a water dimer on the reaction is not significant when compared with the effect of one water molecule.

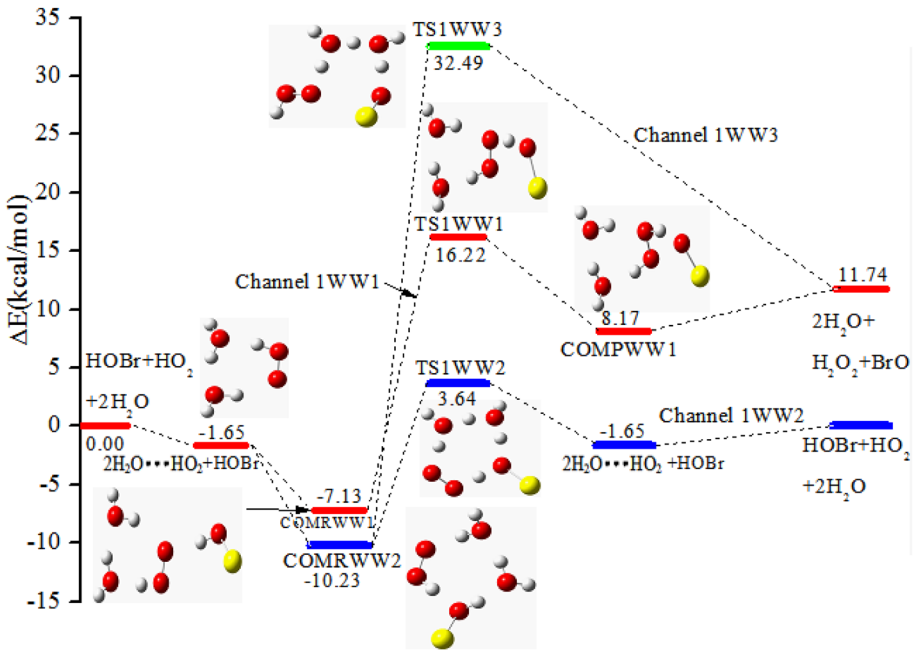

Fig. 5 The PES of the HOBr + HO_2 reaction in the presence of a water dimer *via* the $2H_2O$···HO_2 + HOBr channel at the CCSD(T)/cc-pVTZ//B3LYP/6-311++G(d.p) level of theory (energies in kcal mol^{-1}).

Table 3 Kinetic results for the formation of H_2O_2 + BrO from the HO_2 + HOBr reaction in the absence of water, the presence of a single water molecule and the presence of two water molecules over the temperature range of 216.7–298.2 K at different heights in the Earth's atmosphere

h (km)	T	k_{TS1}	k_{TS1W1}	k_{TS1W2}	k_{TS1W3A}	k_{TS1W3B}	k_{TS1W4}	k_{TS1W5}	k_{TS1WW2}
0	298.15	3.95×10^{-30}	1.83×10^{-28}	5.59×10^{-31}	6.21×10^{-40}	3.28×10^{-42}	1.50×10^{-18}	9.92×10^{-28}	8.32×10^{-22}
0	288.19	1.20×10^{-30}	6.23×10^{-29}	1.70×10^{-31}	1.01×10^{-40}	4.31×10^{-43}	1.40×10^{-18}	3.64×10^{-28}	5.90×10^{-22}
2	275.21	2.22×10^{-31}	1.38×10^{-29}	3.15×10^{-32}	7.71×10^{-42}	2.46×10^{-44}	1.26×10^{-18}	8.93×10^{-29}	3.64×10^{-22}
4	262.23	3.50×10^{-32}	2.64×10^{-30}	4.94×10^{-33}	4.63×10^{-43}	1.07×10^{-45}	1.14×10^{-18}	1.91×10^{-29}	2.16×10^{-22}
6	249.25	4.56×10^{-33}	4.23×10^{-31}	6.44×10^{-34}	2.07×10^{-44}	3.34×10^{-47}	1.01×10^{-18}	3.48×10^{-30}	1.20×10^{-22}
8	236.27	4.78×10^{-35}	5.59×10^{-32}	6.72×10^{-35}	6.59×10^{-46}	7.23×10^{-49}	8.88×10^{-19}	5.29×10^{-31}	6.34×10^{-23}
10	223.29	3.85×10^{-36}	5.85×10^{-33}	5.42×10^{-36}	1.41×10^{-47}	9.96×10^{-51}	7.74×10^{-19}	6.47×10^{-32}	3.13×10^{-23}
12	216.69	9.58×10^{-36}	1.68×10^{-33}	1.34×10^{-36}	1.66×10^{-48}	9.25×10^{-52}	7.20×10^{-19}	2.01×10^{-32}	2.10×10^{-23}

3.4 Kinetics

In addition to investigating the mechanism in the absence of water and in the presence of one water molecule and water dimer molecules, another principal purpose of the study was to investigate the influence of water on the dynamics of the generation of BrO + H_2O_2 from the HOBr + HO_2 reaction. With an increase in altitude, there is a decrease in the rate constants (see Table 3). Table 3 reveals that the rate coefficients of channel 1W1 (k_{TS1W1}), channel 1W4 (k_{TS1W4}) and channel 1W5 (k_{TS1W5}) for the $H_2O\cdots HO_2$ + HOBr, $H_2O\cdots$HOBr + HO_2 and HOBr$\cdots H_2O$ + HO_2 reactions are larger than for the generation of H_2O_2 + BrO in the absence of a water molecule (channel 1, k_{TS1}) at between 216.7 and 298.2 K. The corresponding ratios of k_{TS1W1}/k_{TS1}, k_{TS1W4}/k_{TS1} and k_{TS1W5}/k_{TS1} are in the range of 1.75×10^2 to 4.63×10^1, 7.52×10^{16} to 3.80×10^{11} and 2.10×10^3 to 2.51×10^2, respectively. However, the rate coefficients of channel 1W2 (k_{TS1W2}), channel 1W3A (k_{TS1W3A}) and channel 1W3B (k_{TS1W3B}) for the reactions of $H_2O\cdots HO_2$ + HOBr and $H_2O\cdots$HOBr + HO_2 are smaller than for the reaction in the absence of water (channel 1, k_{TS1}). The ratios of k_{TS1W2}/k_{TS1}, k_{TS1W3A}/k_{TS1} and k_{TS1W3B}/k_{TS1} are 1.40×10^{-1} to 1.42×10^{-1}, 1.73×10^{-13} to 1.57×10^{-10} and 9.66×10^{-17} to 8.30×10^{-13}, respectively. These results show that the presence of water has a positive influence on accelerating the rate of channel 1W1, channel 1W4 and channel 1W5. Yet, other channels contribute less to the enhancement of the title reaction. Moreover, the calculated rate coefficients for channel 1W4 (k_{TS1W4}) are much larger than those of the channel 1W2 (k_{W2}) and channel 1W3 (k_{W3A} and k_{W3B}), and the ratio of k_{TS1W4}/k_{TS1W2}, k_{TS1W4}/k_{TS1W3A} and k_{TS1W4}/k_{TS1W3B} are 5.37×10^{17} to 2.68×10^{12}, 4.34×10^{29} to 2.42×10^{21} and 7.78×10^{32} to 4.57×10^{23}, respectively, which reveals that channel 1W4 will occur more easily. With the addition of a water dimer, as shown in Table 3, the rate constants of channel 1WW2 are 12–8 orders of magnitude higher than the reaction path without water, which is consistent with the HOBr + HCl reaction.[34] However, these rate constants are 4–3 orders of magnitude smaller than those of reactions in the presence of one water molecule. Therefore, the reaction channels in the presence of a water dimer are not as fast as the channels with only one water molecule.

For the sake of a more thorough understanding of the effect of water on the HOBr + HO_2 reaction, we compared the rate of the reaction in the absence of water with the corresponding effective rates in the presence of water. The rate of the reaction in the absence of water is computed according to the equation $v_{R1} = k_{R1}[\text{HOBr}][HO_2]$, while the rates of channel 1W1, channel 1W2, channel 1W3A, channel 1W3B, channel 1W4 and channel 1W5 in the presence of water are computed according to the following equations, respectively.

$$v_{W1} = k_{TS1W1}[HO_2\cdots H_2O][\text{HOBr}] = k'_{TS1W1}[\text{HOBr}][HO_2]$$

$$v_{W2} = k_{TS1W2}[HO_2\cdots H_2O][\text{HOBr}] = k'_{TS1W2}[\text{HOBr}][HO_2]$$

$$v_{W3A} = k_{TS1W3A}[H_2O\cdots\text{HOBr}][HO_2] = k'_{TS1W3A}[\text{HOBr}][HO_2]$$

$$v_{W3B} = k_{TS1W3B}[H_2O\cdots\text{HOBr}][HO_2] = k'_{TS1W3B}[\text{HOBr}][HO_2]$$

$$v_{W4} = k_{TS1W4}[\text{HOBr}\cdots H_2O][HO_2] = k'_{TS1W4}[\text{HOBr}][HO_2]$$

$$v_{W5} = k_{TS1W5}[H_2O\cdots\text{HOBr}][HO_2] = k'_{TS1W5}[\text{HOBr}][HO_2]$$

$$v_{WW2} = k_{TS1WW2}[2H_2O\cdots HO_2][\text{HOBr}] = k'_{TS1WW2}[\text{HOBr}][HO_2]$$

The effective rate constants k'_{TS1W1}, k'_{TS1W2}, k'_{TS1W3A}, k'_{TS1W3B}, k'_{TS1W4}, k'_{TS1W5} and k'_{TS1WW2} are calculated utilizing the water concentration at given temperatures. The amount of water vapor is dependent on the temperature and in general reduces with altitude. At 100% relative humidity, at 298.15 K, the calculated water vapor concentration is 7.2×10^{17} molecules per cm^3.[35] In the above equations,

$$k'_{TS1W1} = k_{TS1W1}K_{eq}(H_2O\cdots HO_2)[H_2O],$$

$$k'_{TS1W2} = k_{TS1W2}K_{eq}(H_2O\cdots HO_2)[H_2O],$$

$$k'_{TS1W3A} = k_{TS1W3A}K_{eq}(H_2O\cdots\text{HOBr})[H_2O],$$

Table 4 Effective rate coefficients for the HO_2 + HOBr + H_2O and HO_2 + HOBr + $2H_2O$ reactions over the temperature range of 216.69–298.15 K (cm^3 per molecule per s) at different heights in the Earth's atmosphere

h (km)	T	$[H_2O]$	$[2H_2O]$	k'_{TS1W1}	k'_{TS1W2}	k'_{TS1W3A}	k'_{TS1W3B}	k'_{TS1W4}	k'_{TS1W5}	k'_{TS1WW2}
0	298.15	7.79×10^{17}	3.1×10^{14}	5.39×10^{-31}	1.65×10^{-33}	3.61×10^{-43}	1.91×10^{-45}	8.73×10^{-22}	1.25×10^{-33}	2.10×10^{-37}
0	288.19	4.34×10^{17}	1.2×10^{14}	1.60×10^{-31}	4.36×10^{-34}	4.69×10^{-44}	2.00×10^{-46}	6.50×10^{-22}	3.05×10^{-34}	6.36×10^{-38}
2	275.21	1.89×10^{17}	2.8×10^{13}	2.90×10^{-32}	6.61×10^{-35}	2.58×10^{-45}	8.23×10^{-48}	4.22×10^{-22}	4.20×10^{-35}	1.05×10^{-38}
4	262.23	7.43×10^{16}	5.7×10^{12}	4.37×10^{-33}	8.19×10^{-36}	1.06×10^{-46}	2.45×10^{-49}	2.61×10^{-22}	4.67×10^{-36}	1.48×10^{-39}
6	249.25	2.64×10^{16}	9.6×10^{11}	5.36×10^{-34}	8.16×10^{-37}	3.11×10^{-48}	5.02×10^{-51}	1.52×10^{-22}	4.12×10^{-37}	1.62×10^{-40}
8	236.27	8.15×10^{15}	1.3×10^{11}	5.10×10^{-35}	6.13×10^{-38}	6.02×10^{-50}	6.60×10^{-53}	8.11×10^{-23}	2.72×10^{-38}	1.40×10^{-41}
10	223.29	2.15×10^{15}	1.3×10^{10}	3.66×10^{-36}	3.39×10^{-39}	7.28×10^{-52}	5.14×10^{-55}	3.99×10^{-23}	1.28×10^{-39}	8.46×10^{-43}
12	216.69	1.01×10^{15}	3.7×10^{9}	8.35×10^{-37}	6.66×10^{-40}	6.14×10^{-53}	3.42×10^{-56}	2.66×10^{-23}	2.31×10^{-40}	1.81×10^{-43}

$$k'_{TS1W3B} = k_{TS1W3B} K_{eq}(H_2O\cdots HOBr)[H_2O],$$

$$k'_{TS1W4} = k_{TS1W4} K_{eq}(H_2O\cdots HOBr)[H_2O],$$

$$k'_{TS1W5} = k_{TS1W5} K_{eq}(HOBr\cdots H_2O)[H_2O]$$

and

$$k'_{TS1WW2} = k_{TS1WW2} K_{eq}(2H_2O\cdots HO_2)[2H_2O],$$

$K_{eq}(H_2O\cdots HO_2)$, $K_{eq}(H_2O\cdots HOBr)$ and $K_{eq}(HOBr\cdots H_2O)$ are the equilibrium constants for the generation of the complexes $H_2O\cdots HO_2$, $H_2O\cdots HOBr$ and $HOBr\cdots H_2O$, respectively. $[H_2O]$ represents the concentration of water. $K_{eq}(2H_2O\cdots HO_2)$ is the equilibrium constant for the generation of the complex $2H_2O\cdots HO_2$, and $[2H_2O]$ represents the concentration of the water dimer. The values for $K_{eq}(H_2O\cdots HO_2)$, $K_{eq}(H_2O\cdots HOBr)$, $K_{eq}(HOBr\cdots H_2O)$ and $K_{eq}(2H_2O\cdots HO_2)$ are listed in Table S1 of the ESI.†

Table 4 reveals the effective rate coefficients of the reaction in the presence of a water molecule and water dimer at different altitudes in the Earth's atmosphere. With the increase in altitude, there is a decrease in the rate constants as the concentrations of water and the water dimer decrease. The concentration of the water dimer is more sensitive to temperature, decreasing by five orders of magnitude as the temperature drops from 298.15 K to 216.69 K. As revealed in Table 4, the effective rate coefficients for channel 1W4 ($k'_{TS1W4} = 2.66 \times 10^{-23} - 8.73 \times 10^{-22}$ cm^3 per molecule per s) are the largest in comparison to channel 1W1, channel 1W2, channel 1W3A, channel 1W3B and channel 1W5. The ratios of k'_{TS1W4}/k'_{TS1W1}, k'_{TS1W4}/k'_{TS1W2}, k'_{TS1W4}/k'_{TS1W3A}, k'_{TS1W4}/k'_{TS1W3B} and k'_{TS1W5}/k'_{TS1W4} are in the range of 3.19×10^{13} to 1.62×10^{9}, 3.99×10^{16} to 5.29×10^{11}, 4.33×10^{29} to 2.42×10^{21}, 7.78×10^{32} to 4.57×10^{23} and 1.15×10^{17} to 6.98×10^{11}, respectively, which demonstrates that channel 1W4 represents a water-assisted reaction. Moreover, k'_{TS1W4} is larger than the rate coefficient of the corresponding channel for the reaction in the absence of water by 12–8 orders of magnitude, suggesting that the water molecule in the $H_2O\cdots HOBr$ + HO_2 pathway has a positive effect on accelerating the rate of the HOBr + HO_2 reaction. As seen in Table 4, the effective rate constants for the reaction involving a water dimer are smaller than both those of the dominant channel, channel 1W4, for the reactions with a single water molecule and the reaction in the absence of water over the temperature range of 216.69–298.15. Therefore, the effect of the water dimer is negative over the investigated temperatures due to the decreased reaction rate constants.

We also calculated the reverse rate constants for the bimolecular addition reaction and unimolecular transformation for HOBr + HO_2 in both the absence and presence of a water molecule and in the presence of a water dimer. The calculated results are presented in Tables S3–S6.† The reverse rate constants and the effective reverse rate constants of the HO_2 + HOBr reaction in the absence of water, in the presence of a single water molecule and two water molecules are higher than of the rate constants of the forward reaction. These are mainly due to the barrier heights of the forward reactions are higher than those of the reverse reactions. For example, the barrier height of the forward reaction for channel 1W4 is 11.99 kcal mol^{-1} and it is 9.79 kcal mol^{-1} for the reverse reaction.

3.5 Atmospheric implications of HOBr

The atmospheric lifetime (τ) of HOBr can be deduced by means of the following formula: $\tau = \frac{1}{k_{[HO_2]}[HO_2]}$. The values used were a mean atmospheric concentration of HO_2 of 4.2×10^4 molecules per cm^3,[36] $k_{[HO_2]} = 3.95 \times 10^{-30}$ cm^3 per molecule per s in the absence of a water molecule and $k_{[HO_2]} = 1.50 \times 10^{-18}$ cm^3 per molecule per s in the presence of one water molecule. The atmospheric lifetime of HOBr is approximately 1.90×10^{17} years in the absence of a water molecule, which is much higher than that in the presence of one water molecule (503.3 years). These results suggest that water molecules have a positive catalytic influence on the HO$_2$ + HOBr reaction, and that the HO_2-initiated reaction of HOBr in the absence and presence of a water molecule are very friendly to the environment.

4. Conclusions

A single water molecule has been demonstrated to take an effective role in accelerating the HOBr + HO_2 reaction. Three kinds of reaction pathways were discovered in the absence of a water molecule. These pathways are determined by how HO_2 approaches HOBr, and the channel that generates H_2O_2 + BrO dominates the whole reaction. In the presence of water, five entrance channels were found. Based on the results, the channel for the reaction

$H_2O\cdots HOBr + HO_2 \rightarrow TS1W4 \rightarrow H_2O + HOBr + HO_2$ might be of great advantage for atmospheric chemistry. The other pathways studies may be ignored owing to their high barrier heights. The rate coefficients and the effective rate coefficients of the reaction in the presence of a water molecule are higher by 16–11 and 12–8 orders of magnitude than those in the absence of water over a range of 216.69–298.15 K, respectively. The rate coefficients of the reaction in the presence of a water dimer are higher than those in the absence of water. Meanwhile, the effective rate coefficients for the reaction in the presence of a water dimer are smaller than those in the absence of water. Consequently, the current investigations clearly show that a single water molecule has a positive catalytic influence on the $HOBr + HO_2$ reaction.

Author contributions

Yongguo Liu, Meilian Zhao, and Yuxi Sun: calculation, data curation, formal analysis, and investigation. Yunju Zhang and Shuxin Liu: calculation, and writing-review and editing.

Conflicts of interest

The authors declare that they have no known competing financial interests or personal relationships that could have appeared to influence the work reported in this paper.

Acknowledgements

This work was supported by the Natural Science Foundations of China (No. 21707062), Scientific Research Starting Foundation of Mianyang Normal University (No. QD2016A007), the Open Project Program of Beijing Key Laboratory of Flavor Chemistry, and the Beijing Technology and Business University (BTBU), Beijing 100048, China.

References

1 A. R. Douglass, S. E. Strahan and R. S. Stolarski, *Agu Fall Meeting AGU Fall Meeting Abstracts*, 2012.
2 J. Langner, M. Engardt and A. Baklanov, *et al.*, *EGU General Assembly Conference Abstracts*, 2012.
3 J. J. Orlando and G. S. Tyndall, *Chem. Soc. Rev.*, 2012, **41**, 6294.
4 N. Kaltsoyannis and D. M. Rowley, *Phys. Chem. Chem. Phys.*, 2002, **4**, 419–427.
5 K. Hebestreit, J. Stutz, D. Rosen, V. Matveiv, M. Peleg, M. Luria and U. Platt, *Science*, 1999, **283**, 55–57.
6 L. Wang, J. Y. Liu, Z. S. Li and C. C. Sun, *J. Comput. Chem.*, 2004, **25**, 558–564.
7 P. S. Monks, F. L. Nesbitt, M. Scanlon and L. J. Stief, *J. Phys. Chem.*, 1993, **97**, 11699–11705.
8 G. Dixon-Lewis, P. Marshall, B. Ruscic, A. Burcat, E. Goos, A. Cuoci, A. Frassoldati, T. Faravelli and P. Glarborg, *Combust. Flame*, 1999, **283**, 55–57.
9 M. E. Jenkin, M. D. Hurley and T. J. Wallington, *J. Phys. Chem. A*, 2010, **114**, 408–416.
10 C. B. Gross, T. J. Dillon, G. Schuster, J. Lelieveld and J. N. Crowley, *J. Phys. Chem. A*, 2014, **118**, 974–985.
11 Z. L. Yang, X. X. Lin, J. C. Zhou, M. F. Hu, Y. B. Gai, W. X. Zhao, B. Long and W. J. Zhang, *RSC Adv.*, 2019, **9**, 40437–40444.
12 Z. L. Yang, X. X. Lin, B. Long and W. J. Zhang, *Chem. Phys. Lett.*, 2020, **749**, 137442.
13 G. Dixon-Lewis, P. Marshall, B. Ruscic, A. Burcat, E. Goos, A. Cuoci, A. Frassoldati, T. Faravelli and P. Glarborg, *Combust. Flame*, 2012, **159**, 528–540.
14 Y. Tanaka, M. Kawasaki, Y. Matsumi, H. Fujiwara, T. Ishiwata, L. J. Rogers, R. N. Dixonand and M. N. R. Ashfold, *J. Chem. Phys.*, 1998, **109**, 1315–1323.
15 J. Gonzalez, J. M. Anglada, R. J. Buszek and J. S. Francisco, *J. Am. Chem. Soc.*, 2011, **133**, 3345–3353.
16 J. Y. Li, N. T. Tsona and L. Du, *Phys. Chem. Chem. Phys.*, 2018, **20**, 10650–10659.
17 S. Aloisio and J. S. Francisco, *J. Phys. Chem. A*, 1998, **102**, 1899–1902.
18 B. Long, X. F. Tan, Z. W. Long, Y. B. Wang, D. S. Ren and W. J. Zhang, *J. Phys. Chem. A*, 2011, **115**, 6559–6567.
19 F. M. Tao, K. Higgins, W. Klemperer and D. D. Nelson, *Geophys. Res. Lett.*, 1996, **23**, 1797.
20 D. Stone and D. M. Rowley, *Phys. Chem. Chem. Phys.*, 2005, **7**, 2156–2163.
21 J. Gonzalez and J. M. Anglada, *J. Phys. Chem. A*, 2010, **114**, 9151–9162.
22 J. M. Anglada and J. Gonzalez, *ChemPhysChem*, 2009, **10**, 3034–3045.
23 Y. Luo, S. Maedaand and K. Ohno, *Chem. Phys. Lett.*, 2009, **469**, 57–61.
24 S. Jorgensen and H. G. Kjaergaard, *J. Phys. Chem. A*, 2010, **114**, 4857–4863.
25 T. L. Zhang, W. L. Wang, P. Zhang, J. Lu and Y. Zhang, *Phys. Chem. Chem. Phys.*, 2011, **13**, 20794–20805.
26 A. D. Becke, *J. Chem. Phys.*, 1993, **98**, 5648.
27 Y. Z. Tang, H. F. Sun, J. Zhao, J. H. Liu and R. S. Wang, *Atmos. Environ.*, 2013, **65**, 164–170.
28 C. Gonzalez and H. B. Schlegel, *J. Chem. Phys.*, 1989, **90**, 2154–2161.
29 C. Gonzalez and H. B. Schlegel, *J. Phys. Chem.*, 1990, **94**, 5523–5527.
30 K. Raghavachari, G. W. Trucks, J. A. Pople and M. Head-Gordon, *Chem. Phys. Lett.*, 1989, **157**, 479–483.
31 M. J. Frisch, G. W. Trucks, H. B. Schlegel, G. E. Scuseria, M. A. Robb, J. R. Cheeseman, G. Scalmani, V. Barone, B. Mennucci, G. A. Petersson, H. Nakatsuji, M. Caricato, X. Li, H. P. Hratchian, A. F. Izmaylov, J. Bloino, G. Zheng, J. L. Sonnenberg, M. Hada, M. Ehara, K. Toyota, R. Fukuda, J. Hasegawa, M. Ishida, T. Nakajima, Y. Honda, O. Kitao, H. Nakai, T. Vreven, J. A. Montgomery Jr, J. E. Peralta, F. Ogliaro, M. Bearpark, J. J. Heyd, E. Brothers, K. N. Kudin, V. N. Staroverov, R. Kobayashi, J. Normand, K. Raghavachari, A. Rendell, J. C. Burant, S. S. Iyengar, J. Tomasi, M. Cossi, N. Rega, J. M. Millam, M. Klene, J. E. Knox, J. B. Cross, V. Bakken, C. Adamo, J. Jaramillo, R. Gomperts, R. E. Stratmann, O. Yazyev,

A. J. Austin, R. Cammi, C. Pomelli, J. W. Ochterski, R. L. Martin, K. Morokuma, V. G. Zakrzewski, G. A. Voth, P. Salvador, J. J. Dannenberg, S. Dapprich, A. D. Daniels, O. Farkas, J. B. Foresman, J. V. Ortiz, J. Cioslowski and D. J. Fox, Gaussian, Inc., Wallingford CT, 2009.

32 S. Canneaux, F. Bohr and E. Henon, *J. Comput. Chem.*, 2014, **35**, 82–93.

33 A. Shiroudi and M. S. Deleuze, *J. Phys. Chem. A*, 2014, **118**, 4593–4610.

34 A. F. Voegele, C. S. Tautermann, T. Loerting and K. R. Liedl, Reactions of HOBr + HCl + nH_2O and HOBr + HBr + nH_2O, *Chem. Phys. Lett.*, 2003, **372**, 569–576.

35 J. M. Anglada, R. Crehuet, M. Martins-Costa, J. S. Francisco and M. Ruiz-Lopez, The atmospheric oxidation of CH_3OOH by the OH radical: the effect of water vapor, *Phys. Chem. Chem. Phys.*, 2017, **19**, 12331–12342.

36 S. C. Smith, J. D. Lee, W. J. Bloss, G. P. Johnson, T. Ingham and D. E. Heard, Concentrations of OH and HO2 radicals during NAMBLEX: measurements and steady state analysis, *Atmos. Chem. Phys.*, 2006, **5**, 1435–1453.